Progress In Electromagnetics Research C, Vol. 92, 17–30, 2019

Statistical Broadband over Power Lines Channel Modeling — Part 2: The Numerical Results of the Statistical Hybrid Model

Athanasios G. Lazaropoulos*

Abstract—This second paper presents the numerical evaluation of the statistical hybrid model for a number of indicative overhead medium-voltage (OV MV) and underground medium-voltage (UN MV) broadband over power lines (BPL) topologies. In essence, this paper assesses the effect of a number of key factors already reported in [1], such as the distribution power grid type, BPL topology class, coupling scheme, channel attenuation statistical distribution, and injected power spectral density (IPSD) limits, on the computed capacity ranges of the statistical hybrid model. For the assessment of the different channel attenuation statistical distributions, the graphical analysis and the proposed metrics of capacity percentage change and average absolute capacity percentage change are demonstrated while two rules of thumb estimating the fidelity results are also proposed.

1. INTRODUCTION

The theoretical framework and flowchart of the statistical hybrid model have already been presented in [1] while the inputs, outputs, and required processes of the statistical hybrid model have been detailed there. In brief, the statistical hybrid model is first based on the formality and validity of the well-known deterministic hybrid model which is simply denoted as hybrid model [2–10]. In fact, hybrid model exploits its two interconnected modules, say the bottom-up approach module and top-down approach module, so that channel attenuation results can be computed for given multi-transmission line (MTL) distribution configurations, overhead medium-voltage (OV MV) and underground medium-voltage (UN MV) broadband over power lines (BPL) topologies, and applied coupling schemes. A number of indicative OV MV and UN MV BPL topologies are assumed so that these distribution BPL topologies act as the representative ones of respective BPL topology classes. The inputs of the statistical hybrid model coincide with those of the hybrid model that are the distribution power grid type (either OV MV or UN MV), indicative distribution BPL topology of Tables 1 and 2 of [1], respective distribution MTL configuration, and applied coupling scheme. Second, the statistical hybrid model exploits the Gaussian, Lognormal, Wald, Weibull, and Gumbel channel attenuation distributions of [1], which are based on the respective well-known statistical distributions and are widely used in the communications research fields. By appropriately filtering the channel attenuation results of the hybrid model in terms of the maximum likelihood estimators (MLEs) of the respective indicative BPL topologies, channel attenuation statistical distributions enrich the assumed distribution BPL topology classes with statistically equivalent BPL topologies. Third, statistical hybrid model computes the capacities of all the available BPL topologies for given distribution BPL topology class, electromagnetic interference (EMI) limits, coupling schemes, and noise levels, thus estimating the capacity range of each BPL topology class. All the aforementioned processes are synopsized in the six phases of the statistical hybrid model that are detailed in [1].

Received 29 January 2019, Accepted 28 March 2019, Scheduled 5 April 2019
* Corresponding author: Athanasios G. Lazaropoulos (AGLazaropoulos@gmail.com).
The author is with the School of Electrical and Computer Engineering, National Technical University of Athens, 9, Iroon Polytechneiou Street, GR 15780, Zografou Campus, Athens, Greece.

The rest of this paper is organized as follows. In Section 2, the numerical results of the statistical hybrid model are demonstrated with focus on the impact assessment of the distribution power grid type, t BPL topology class, coupling scheme, channel attenuation statistical distribution, and injected power spectral density (IPSD) limits of EMI limits on the computed capacity ranges of the statistical hybrid model.

2. NUMERICAL RESULTS AND DISCUSSION

In this Section, numerical results concerning the operation of the statistical hybrid model are demonstrated. More specifically, the key factors, which are the distribution power grid type, BPL topology class, coupling scheme, channel attenuation statistical distribution, and IPSD limits, that mainly influence the operation of the statistical hybrid model have already been reported in [1] and are here assessed. In order to execute the performance assessment of the statistical hybrid model, the default operation settings of the statistical hybrid model need to be reported, namely:

- With reference to Tables 1 and 2 of [1], the indicative topologies of OV MV and UN MV BPL networks, as well as their respective MTL configurations, are assumed with the purpose of enriching the respective BPL topology classes. As the members of each BPL topology class are concerned, 100 member distribution BPL topologies (i.e., $P = 100$) are assumed to be added in each BPL topology class per channel attenuation statistical distribution through the statistical hybrid model flowchart described in [1].
- To compute coupling scheme channel attenuation differences of Eq. (5) of [1], the circuital parameters of the hybrid model of Section 2.2 in [1] are first assumed in this paper. Second, the BPL signals are injected into and extracted from the lines by applying the CS2 module as detailed in [8, 10]. Coupling scheme types 1, 2 and 3 are examined in this paper while WtG^1 and StP^1 coupling schemes are assumed to be the default ones for the assessment of OV MV and UN MV BPL topology classes, respectively.
- During the computation of the coupling scheme channel attenuation differences in the Phase B of [1], only positive values are expected while in the scarce cases of negative and zero coupling scheme channel attenuation differences, the coupling scheme channel attenuation differences are assumed to be equal to an arbitrarily low value, say 1×10^{-11}. Instead of zero, the value 1×10^{-11} is assumed so that MLEs of Lognormal, Wald, and Weibull channel attenuation distributions, which comprise natural logarithms and denominators, can be calculated.
- Since FCC Part 15 [11], German Reg TP NB30 [12], and BBC/NATO Proposal [13], which are the IPSD limit proposals concerning EMI policies for BPL systems, are all well defined in the frequency range 3–30 MHz, this frequency range is used in this paper. For the required capacity computations of the statistical hybrid model, the flat-fading subchannel frequency spacing is assumed to be equal to 0.1 MHz (i.e., $f_s = 0.1\,\mathrm{MHz}$) that implies 270 subchannels in the frequency range of interest (i.e., $Q = 270$). FCC Part 15 is assumed to be the default EMI policy in this paper while $-60\,\mathrm{dBm/Hz}$ and $-40\,\mathrm{dBm/Hz}$ are the FCC Part 15 IPSD limits $p(\cdot)$ suitable for the operation of OV MV and UN MV BPL topologies, respectively [4, 6, 14].

During the capacity computations, uniform additive white Gaussian noise (AWGN) PSD levels are assumed in accordance with the FL noise model of [15, 16]. As the noise properties of OV MV and UN MV BPL networks are regarded in the 3–30 MHz frequency range [4, 6, 17–19], $-105\,\mathrm{dBm/Hz}$ and $-135\,\mathrm{dBm/Hz}$ are the appropriate AWGN PSD limit levels $N(\cdot)$ for OV MV and UN MV BPL networks, respectively.

2.1. OV MV and UN MV MTL Configurations

As the default operation settings have already been presented and assumed, in Table 1, MLEs of the Gaussian, Lognormal, Wald, Weibull, and Gumbel channel attenuation distributions are reported for the indicative OV MV BPL topologies of Table 1 of [1] while in Table 2, MLEs of the aforementioned channel attenuation distributions are reported for the indicative UN MV BPL topologies of Table 2 of [1].

From Tables 1 and 2, several initial observations can be made concerning the MLE computation of the statistical hybrid model during the default operation settings, namely:

- As the complexity of the BPL topologies increases so do $\hat{\mu}_{\text{MLE}}^{\text{Gaussian}}$, $\hat{\mu}_{\text{MLE}}^{\text{Lognormal}}$, $\hat{\mu}_{\text{MLE}}^{\text{Wald}}$, $\hat{a}_{\text{MLE}}^{\text{Weibull}}$ and $\hat{a}_{\text{MLE}}^{\text{Gumbel}}$ regardless of the examined power grid type. High complexity implies that BPL topology is characterized by a rich multipath environment that further implies high coupling scheme channel attenuation differences $\Delta\mathbf{A}_{l,1}^{\text{G,C}}(\mathbf{f})$ in Phase B of [1]. Since MLE computation of Phase C of [1] is based on the coupling scheme channel attenuation differences, which assess the channel attenuation difference between the examined BPL topology and respective distribution "LOS" topology, the aforementioned MLEs of urban BPL topologies present higher values than the ones of suburban, rural, and "LOS" topologies in all the cases examined. Same results also occur for $\hat{\sigma}_{\text{MLE}}^{\text{Gaussian}}$, $\hat{\sigma}_{\text{MLE}}^{\text{Lognormal}}$, $\hat{\lambda}_{\text{MLE}}^{\text{Wald}}$, $\hat{\beta}_{\text{MLE}}^{\text{Weibull}}$ and $\hat{\epsilon}_{\text{MLE}}^{\text{Gumbel}}$.

Table 1. MLEs of channel attenuation statistical distributions of indicative OV MV BPL topologies for default operation settings (say, $\text{WtG}^1/\text{StP}^1$ coupling scheme).

Topology Name	**BPL Topology Class Description**	**Gaussian MLEs**		**Lognormal MLEs**		**Wald MLEs**		**Weibull MLEs**		**Gumbel MLEs**	
		$\hat{\mu}_{\text{MLE}}^{\text{Gaussian}}$	$\hat{\sigma}_{\text{MLE}}^{\text{Gaussian}}$	$\hat{\mu}_{\text{MLE}}^{\text{Lognormal}}$	$\hat{\sigma}_{\text{MLE}}^{\text{Lognormal}}$	$\hat{\mu}_{\text{MLE}}^{\text{Wald}}$	$\hat{\lambda}_{\text{MLE}}^{\text{Wald}}$	$\hat{\alpha}_{\text{MLE}}^{\text{Weibull}}$	$\hat{\beta}_{\text{MLE}}^{\text{Weibull}}$	$\hat{\alpha}_{\text{MLE}}^{\text{Gumbel}}$	$\hat{\epsilon}_{\text{MLE}}^{\text{Gumbel}}$
Urban case A	Typical OV MV BPL urban topology class	12.78	11.51	1.71	3.47	12.78	6.78×10^{-10}	12.21	0.88	7.64	7.84
Urban case B	Aggravated OV MV BPL urban topology class	17.83	13.31	2.53	0.970	17.83	10.54	19.40	1.34	9.73	11.92
Suburban case	OV MV BPL suburban topology class	7.49	9.64	1.06	2.67	7.49	1.36×10^{-9}	6.44	0.76	5.03	3.97
Rural case	OV MV BPL rural topology class	3.06	3.02	0.27	2.94	3.06	9.03×10^{-10}	2.82	0.83	2.04	1.71
"LOS" case	OV MV BPL "LOS" transmission class	1×10^{-11}	0	-25.33	4×10^{-15}	1×10^{-11}	2.62×10^{3}	1×10^{-11}	∞	1×10^{-3}	1×10^{-11}

Table 2. MLEs of channel attenuation statistical distributions of indicative UN MV BPL topologies.

Topology Name	**BPL Topology Class Description**	**Gaussian MLEs**		**Lognormal MLEs**		**Wald MLEs**		**Weibull MLEs**		**Gumbel MLEs**	
		$\hat{\mu}_{\text{MLE}}^{\text{Gaussian}}$	$\hat{\sigma}_{\text{MLE}}^{\text{Gaussian}}$	$\hat{\mu}_{\text{MLE}}^{\text{Lognormal}}$	$\hat{\sigma}_{\text{MLE}}^{\text{Lognormal}}$	$\hat{\mu}_{\text{MLE}}^{\text{Wald}}$	$\hat{\lambda}_{\text{MLE}}^{\text{Wald}}$	$\hat{\alpha}_{\text{MLE}}^{\text{Weibull}}$	$\hat{\beta}_{\text{MLE}}^{\text{Weibull}}$	$\hat{\alpha}_{\text{MLE}}^{\text{Gumbel}}$	$\hat{\epsilon}_{\text{MLE}}^{\text{Gumbel}}$
Urban case A	Typical UN MV BPL urban topology class	10.58	7.81	2.14	0.64	10.58	20.93	11.85	1.51	4.76	7.42
Urban case B	Aggravated UN MV BPL urban topology class	19.96	8.17	2.90	0.47	19.96	80.22	22.48	2.63	7.20	16.02
Suburban case	UN MV BPL suburban topology class	7.04	2.73	1.85	0.49	7.04	24.70	7.90	2.80	2.64	5.67
Rural case	UN MV BPL rural topology class	3.54	1.23	1.21	0.35	3.54	27.14	3.95	2.84	1.02	3.00
"LOS" case	UN MV BPL "LOS" transmission class	1×10^{-11}	0	-25.33	4×10^{-15}	1×10^{-6}	2.62×10^{3}	1×10^{-11}	∞	1×10^{-3}	1×10^{-11}

- As already mentioned, the value of 1×10^{-11} is used instead of zero so that divisions by zero during the MLE computation of Lognormal, Wald and Weibull channel attenuation distribution are avoided. Due to this assumption, MLEs are observed in OV MV and UN MV "LOS" cases that have rather a compromise character. Anyway, in accordance with the definition of the statistical hybrid model, the OV MV and UN MV BPL topology classes of "LOS" case consist of only one BPL topology each, say the indicative OV MV and UN MV "LOS" cases of the respective Tables 1 and 2 of [1]. Hence, "LOS" cases are not examined in the rest of the paper since the results of the statistical hybrid model coincide with the ones of the hybrid model and do not offer useful statistical findings except for their deterministic capacity output of the hybrid model.

Since MLEs of each channel attenuation statistical distribution for all the indicative BPL topology classes for given power grid type and coupling scheme are available in Tables 1 and 2, respectively, each BPL topology class is enriched with 100 topology members per channel attenuation statistical distribution through the random number generator of Phase D, whose operation has been described in [1]. Then, Phase E determines the coupling scheme transfer function of the members of each BPL topology class for given power grid type, coupling scheme, and channel attenuation statistical distribution while Phase F computes the maximum, average, and minimum capacities of each BPL topology class among its 100 BPL topology members for given power grid type, coupling scheme, channel attenuation statistical distribution, and EMI policy. In Fig. 1(a), the maximum, average, and minimum capacities of the typical OV MV urban topology class are plotted for the Gaussian, Lognormal, Wald, Weibull, and Gumbel channel attenuation distributions when the default operation settings of the statistical hybrid model are considered. Also, the capacity of the indicative BPL topology of the BPL topology class, say, OV MV urban case A, which is computed by the hybrid model, is used as the base value of the figure. In Figs. 1(b)–1(d), same bar graphs are demonstrated with Fig. 1(a) but for the aggravated OV MV BPL urban topology class, OV MV BPL suburban topology class, and OV MV BPL rural topology class, respectively. Figs. 2(a)–2(d) are the same as Figs. 1(a)–1(d), respectively but for the UN MV BPL topology classes.

The behavior of channel attenuation statistical distribution MLEs of Tables 1 and 2 is reflected on the respective Figs. 1 and 2, namely:

- Capacity ranges of the different channel attenuation statistical distributions mainly depend on the examined distribution power grid type. Actually, capacity ranges of the UN MV BPL topology classes are significantly narrower than those of the OV MV BPL topology classes regardless of the applied channel attenuation statistical distribution. This is because distance rather than multipath is identified as the dominant factor affecting signal transmission in most UN MV BPL topologies while the opposite occurs in OV MV BPL topologies, where the effect of multipath is significantly more severe [7]. With reference to Eq. (6) of [1], since the coupling scheme channel transfer function of UN MV BPL topologies mainly depends on the coupling scheme channel transfer function of the UN MV "LOS" case rather on the random number line vector, capacities of UN MV BPL topologies tend to present small differences with respect to the capacity of the "LOS" case. Thus, the capacity ranges of UN MV BPL topology classes are expected to be narrow. The opposite occurs in the case of OV MV BPL topology classes where wider capacity ranges are observed due to the significant role of random number line vector during the computation of the coupling scheme channel transfer function of OV MV BPL topologies.
- Both the following criteria should be satisfied so that a channel attenuation statistical distribution can be considered as acceptable for the statistical hybrid model, namely: (i) capacity range of each distribution BPL topology class comprises the capacity of the respective indicative distribution BPL topology, and (ii) the average capacity value remains very close to the respective one of the indicative distribution BPL topology. On the basis of the previous two criteria:
  - As OV MV BPL topology classes are concerned, only Weibull channel attenuation succeeds in satisfying both the criteria in all the BPL topology classes examined. Gaussian, Lognormal, Wald, and Gumbel fail in one, three, four, and three OV MV BPL topology classes, respectively. More specifically, Lognormal and Gumbel channel attenuation statistical distributions perform well only in the OV MV BPL topology classes of intense multipath environment (i.e., aggravated OV MV BPL urban topology class) while Gaussian channel attenuation statistical distribution performs well in all the OV MV BPL topology classes except for the OV MV

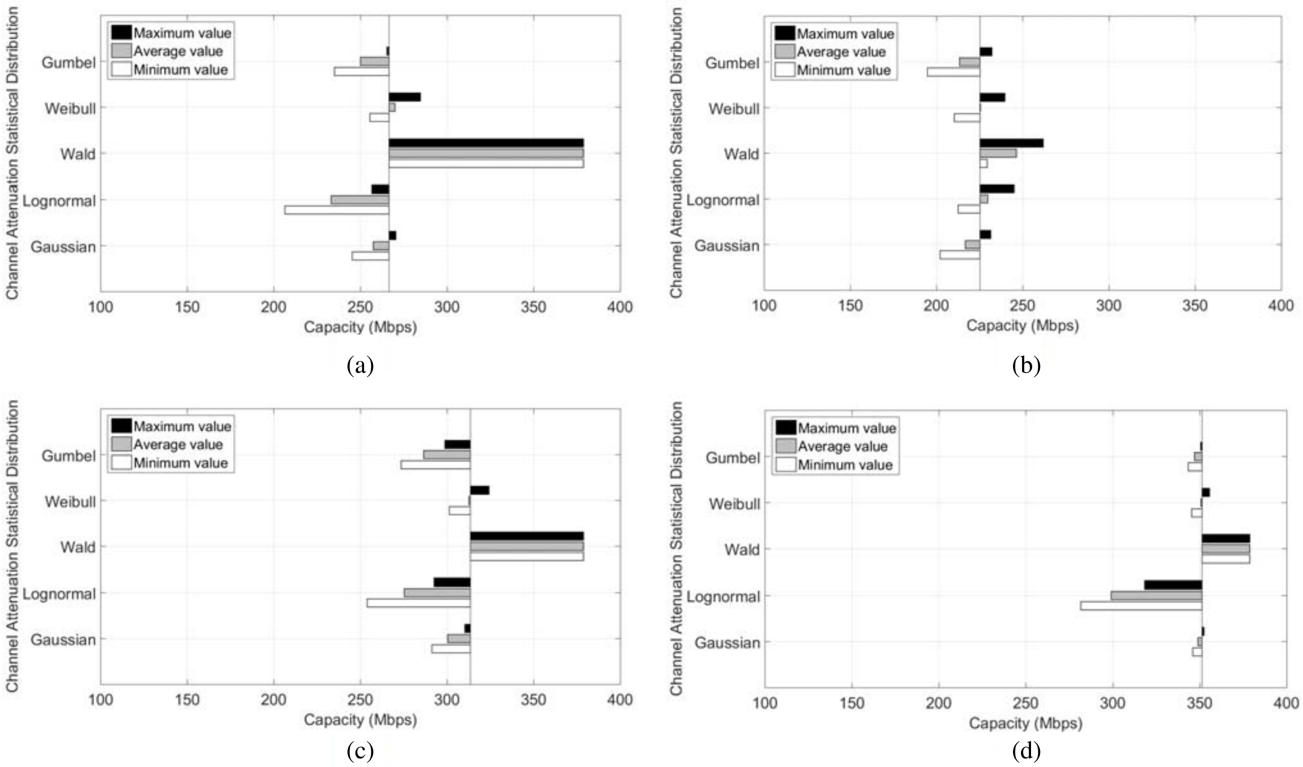

Figure 1. Maximum, average and minimum OV MV BPL topology class capacities for the five examined channel attenuation statistical distributions. (a) Typical OV MV BPL urban topology. (b) Aggravated OV MV BPL urban topology. (c) OV MV BPL suburban topology. (d) OV MV BPL rural topology.

BPL suburban one. Wald channel attenuation statistical distribution fails in successfully estimating capacity for OV MV BPL topology classes due to the combination of low OV MV "LOS" coupling coupling scheme channel transfer function values and the existence of spectral notches.

– As UN MV BPL topology classes are concerned, all the examined channel attenuation statistical distributions succeed in satisfying both the criteria in all the cases examined. All the channel attenuation statistical distributions operate very well regardless of the degree of multipath intensity since high UN MV "LOS" coupling coupling scheme channel transfer function values remain the key element to be fitted.

- Regardless of the examined channel attenuation statistical distribution, when the capacity ranges of a BPL topology class comprise the capacity of the respective indicative topology, the average value of the capacity remains close enough to the capacity of the respective indicative topology in all the cases examined. The opposite occurs when the capacity ranges of a BPL topology class do not comprise the capacity of the respective indicative topology. Hence, there is no need for graphically checking the success degree of the channel attenuation statistical distribution through the capacity ranges and capacity average value but simply setting a capacity percentage threshold that is going to examine the proximity between the average value of the capacity of the examined BPL topology class and the capacity of the respective indicative topology.

To numerically assess the performance of channel attenuation statistical distributions during the operation of the hybrid statistical model and to set the threshold of a successful capacity estimation from a channel attenuation statistical distribution, the percentage change between each average capacity of the distribution BPL topology class and the capacity of the indicative topology of the respective class for the Gaussian, Lognormal, Wald, Weibull, and Gumbel channel attenuation distributions is now proposed and given in Table 3. Also, at the bottom of Table 3, the average absolute percentage change

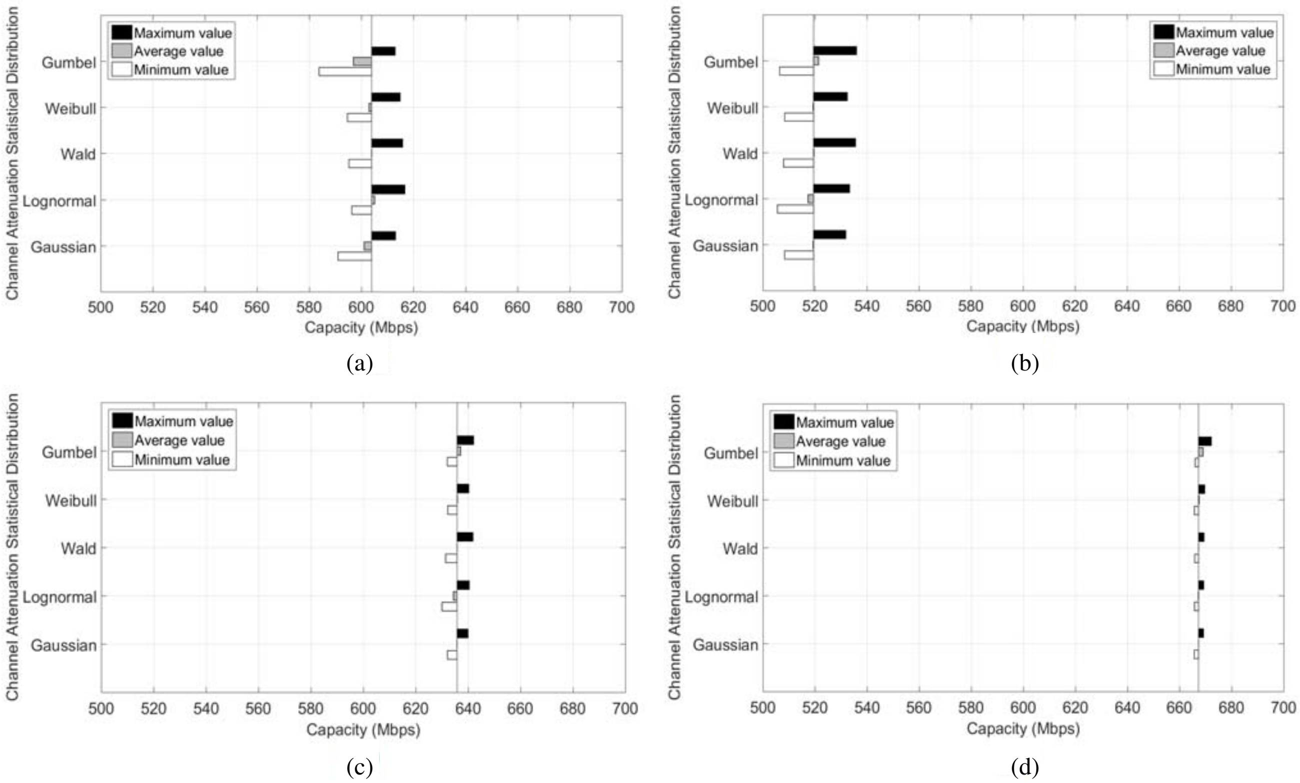

Figure 2. Same curves with Fig. 1 but for the UN MV BPL topology classes.

Table 3. Percentage change between the average capacity of the distribution BPL topology class and the capacity of the indicative topology of the respective class for the five examined channel attenuation statistical distributions and default operation settings (say, $\mathrm{WtG}^1/\mathrm{StP}^1$ coupling scheme and FCC Part 15). (grey background: best results, black background: unsuccessful capacity estimation).

Indicative BPL Topology Name (OV MV Capacity / UN MV Capacity in Mbps)	BPL Topology Class Description	Percentage Change (%)									
		Gaussian		Lognormal		Wald		Weibull		Gumbel	
		OV MV	UN MV	OV MV	UN MV	OV MV	UN MV	OV MV	UN MV	OV MV	UN MV
Urban case A (266 / 604)	Typical BPL urban class	-3.41	-0.48	-12.53	0.19	42.14	0.01	1.32	-0.16	-6.18	-1.16
Urban case B (225 / 519)	Aggravated BPL urban	-3.77	-0.03	2.04	-0.41	9.41	0.02	0.12	-0.03	-5.28	0.37
Suburban case (313 / 636)	BPL suburban class	-4.18	-0.006	-12.18	-0.21	20.84	0.003	-0.26	0.012	-8.62	0.21
Rural case (351 / 667)	BPL rural class	-0.66	-0.001	-14.89	-0.01	7.81	0.0004	-0.16	0.03	-1.25	0.26
Average Absolute Percentage Change (%)		**3.01**	**0.13**	**10.41**	**0.21**	**20.05**	**0.01**	**0.47**	**0.06**	**5.33**	**0.50**

of each channel attenuation statistical distribution is given per power grid type.

The numerical findings presented at Table 3 validate the observations made in Figs. 1(a)–1(d) and 2(a)–2(d), namely:

- High values of percentage change indicate that the capacity estimation is unsuccessful. In accordance with the findings of Figs. 1(a)–1(d) and 2(a)–2(d), all the unsuccessful estimations are demonstrated in black background color in Table 3. Here, a threshold of 3% can be defined so that capacity estimations of percentage change, which remain greater than this threshold in absolute value, can be considered as unsuccessful ones. The rule of thumb of 3% threshold, denoted as first rule of thumb hereafter, is valid in all the cases examined except for the OV MV BPL rural class when Gumbel channel attenuation distribution is applied. Anyway, Gumbel channel attenuation statistical distribution capacity ranges in the OV MV BPL rural class can be marginally considered as unsuccessful ones since the maximum, average, and minimum capacity values remain enough near the respective indicative OV MV BPL topology.

- The metric of the average absolute percentage change indicates the overall capacity performance of the examined channel attenuation statistical distribution. Based on the proposed first rule of thumb, if the average percentage change remains lower than 3% for given power grid type, the examined channel attenuation statistical distribution can provide successful capacity estimations for the BPL topology classes of the examined power grid type. Conversely, average absolute percentage changes that remain higher than 3% entail unsuccessful capacity estimations; the higher the average absolute percentage change remains, the more unsuccessful the capacity estimations per power grid type are made by the channel attenuation statistical distribution.
- Apart from the success of the capacity estimations, the average absolute percentage change assesses the quality of the estimations. More specifically:
  - The lowest average percentage change in absolute value, say 0.12%, of the Weibull channel attenuation statistical distribution among the other distributions for the OV MV power grid type validates the graphical findings and the analysis of Figs. 1(a)–1(d). Anyway, all the average absolute percentage changes of the examined channel attenuation statistical distributions except for the Weibull one remain well above 3%. At the same time, if the percentage change is uniquely examined for each OV MV BPL topology class, Weibull channel attenuation statistical distribution again presents the lowest percentage change among the other channel attenuation statistical distributions. In Table 3, the best percentage change and average percentage change results for the OV MV BPL topology classes of the Weibull channel attenuation statistical distribution are presented in grey background color.
  - The lowest average percentage change, say 0.0004%, of the Wald channel attenuation statistical distribution among the other distributions for the UN MV power grid type validates the graphical findings and the analysis of Figs. 2(a)–2(d). In UN MV power grid, all the examined channel attenuation statistical distributions present average percentage changes significantly lower than the threshold of 3% implying the very successful capacity estimations already recognized from Figs. 2(a)–(d) and the higher competition among the distributions. At the same time, since all the UN MV BPL topology class percentage changes of the examined channel attenuation statistical distributions remain lower than 3%, the two criteria of a successful capacity estimation revealed from Figs. 2(a)–2(d) are here verified. Similar to OV MV BPL topology classes, in Table 3, the best percentage change and average percentage change results for the UN MV BPL topology classes of the Wald channel attenuation statistical distribution are presented in grey background color.

In accordance with the graphical analysis and the percentage change analysis of this Subsection for the default operation settings, UN MV capacity estimations remain more successful than OV MV ones while Weibull and Wald channel attenuation statistical distributions perform the best capacity estimations in OV MV and UN MV power grid types for all the examined BPL topology classes.

2.2. Statistical Hybrid Model, Channel Attenuation Statistical Distributions and EMI Policies

Since OV MV and UN MV BPL networks may become both a source and a victim of EMI, a critical issue related to BPL technology has to do with the EMI policies that should be imposed to ensure the right EMI operation of BPL systems with the one of other already existing wireless and telecommunications systems [4, 6, 17, 20–23]. Among regulatory bodies that have established EMI policies concerning BPL network operation and the corresponding emissions from BPL equipment, three typical EMI policies from national bodies are examined in this paper, namely: FCC Part 15, German Reg TP NB30, and BBC/NATO Proposal. Instead of the formal comprehensive compliance testing procedures that require electromagnetic field measurements at each BPL system, a simpler regulatory approach is applied by limiting IPSD limits to a level that BPL systems do not produce EMI exceeding certain limits in most circumstances. As the EMI policies from national bodies are concerned, the electromagnetic field strength limits proposed by FCC Part 15, German Reg TP NB30, and BBC/NATO Proposal are presented in [13, 20, 23, 24] while the respective IPSD limits $p(\cdot)$ are computed in [13].

Until now, the different channel attenuation statistical distributions of the hybrid statistical model have been assessed when the default operation settings, which comprise FCC Part 15 IPSD limits, are assumed. Since no MTL configuration, BPL topology, and coupling scheme changes occur, the MLEs of channel attenuation statistical distributions of indicative OV MV and UN MV BPL topologies that are reported in the respective Tables 1 and 2 remain the same. With reference to Eqs. (3) and (6) of [1], since the coupling scheme channel attenuation values, which are based on MLEs of Tables 1 and 2, also remain same during the capacity computations for given power grid type, BPL topology class and channel attenuation statistical distribution, the capacity only depends on the applied IPSD limits $p(\cdot)$.

To numerically assess the performance of channel attenuation statistical distributions during the operation of the hybrid statistical model when lower IPSD limits than those of FCC Part 15 are applied, the percentage change between each average capacity of the distribution BPL topology class and the capacity of the indicative topology of the respective class for the same channel attenuation distributions with Table 2 when German Reg TP NB30 is applied is given in Table 4. Similar to Table 3, at the bottom of the table, the average percentage change of each channel attenuation statistical distribution is given per power grid type. In Table 5, same table as Table 4 is given but for the application of BBC/NATO Proposal.

By comparing Tables 4 and 5 with Table 3, it is evident that the success and performance of channel attenuation statistical distributions of the statistical hybrid model drastically depend on the

Table 4. Same with Table 3 but for German Reg TP NB30.

Indicative BPL Topology Name (OV MV Capacity / UN MV Capacity in Mbps)	BPL Topology Class Description	Percentage Change (%)									
		Gaussian		Lognormal		Wald		Weibull		Gumbel	
		OV MV	UN MV	OV MV	UN MV	OV MV	UN MV	OV MV	UN MV	OV MV	UN MV
Urban case A (5.99 / 218)	Typical BPL urban class	1.97	-1.29	67.94	1.05	286.8	0.56	23.52	-0.27	24.01	-2.64
Urban case B (3.93 / 144)	Aggravated BPL urban	8.50	-1.60	1.61	0.09	29.77	1.40	-7.04	-1.37	58.60	0.49
Suburban case (10.75 / 248)	BPL suburban class	-13.76	0.001	9.74	-0.47	115.7	0.08	2.38	0.06	-3.57	0.57
Rural case (14.88 / 280)	BPL rural class	-6.60	-0.001	-5.60	-0.03	55.79	0.0031	1.97	0.08	-9.01	0.62
Average Absolute Percentage Change (%)		**7.71**	**0.72**	**21.22**	**0.41**	**122.2**	**0.51**	**8.73**	**0.44**	**23.80**	**1.08**

Table 5. Same with Table 3 but for BBC/NATO proposal.

Indicative BPL Topology Name (OV MV Capacity / UN MV Capacity in Mbps)	BPL Topology Class Description	Percentage Change (%)									
		Gaussian		Lognormal		Wald		Weibull		Gumbel	
		OV MV	UN MV	OV MV	UN MV	OV MV	UN MV	OV MV	UN MV	OV MV	UN MV
Urban case A (0.0017 / 9.83)	Typical BPL urban class	10.92	14.28	87.67	10.78	354.4	10.02	29.74	12.09	39.70	32.96
Urban case B (0.0011 / 4.65)	Aggravated BPL urban	15.16	-30.91	-2.54	-36.18	25.65	-33.43	-9.32	-35.33	75.73	8.41
Suburban case (0.0032 / 14.28)	BPL suburban class	-11.42	-2.22	14.01	-0.28	136.8	2.11	2.97	-2.05	2.37	3.30
Rural case (0.0045 / 22.09)	BPL rural class	-7.93	0.19	-2.54	0.09	67.80	0.25	2.16	0.71	-9.96	4.36
Average Absolute Percentage Change (%)		**11.36**	**11.90**	**26.69**	**11.83**	**146.2**	**11.45**	**11.05**	**12.54**	**31.94**	**12.26**

applied IPSD limits. Actually, the selection of the more EMI protective to other telecommunication services IPSD limits (i.e., German Reg TP NB30 and BBC/NATO proposal) entail significant capacity reductions either in OV MV or in UN MV BPL systems, which are already highlighted in Tables 4 and 5. Practically, the broadband character of the BPL technology is eliminated when such low IPSD limits are adopted. At the same time, the frequency selective character of German Reg TP NB30 and BBC/NATO proposal should be reminded, which is described in Table 3 of [25], in contrast to FCC Part 15 limits in the 3–30 MHz frequency range. Apart from the low capacities, the reduction of IPSD limits also entails an increase of the number of unsuccessful capacity estimations from channel attenuation statistical distributions that is anyway numerically verified by the increase of average absolute percentage changes regardless of the examined power grid type and channel attenuation statistical distribution. The latter is explained by the fact that the examined channel attenuation statistical distributions create a random number line vector (see Phase D of [1]) across the 3–30 MHz frequency range that is directly subtracted by the coupling scheme channel transfer function of the indicative "LOS" case for given power grid type and coupling scheme. As the IPSD limits become lower and more frequency selective, the frequency locations of the minima and maxima of the random number line vector become important in comparison with the relatively higher IPSD limits of FCC Part 15.

Apart from the general increase of the average absolute percentage change, lower IPSD limits differently affect the capacity estimation in terms of the power grid type and the BPL topology class, namely:

- As already mentioned, the capacity estimation of the channel attenuation statistical distributions remains more successful for the OV MV BPL topology classes when IPSD limits remain high enough. As IPSD limits become lower, the percentage change of all OV MV BPL topology classes increases while capacity estimations of OV MV BPL topology classes that are more prone to multipath transmission (i.e., typical OV MV BPL urban and aggravated OV MV BPL urban classes) become unsuccessful. Actually, Gaussian and Lognormal channel attenuation statistical distributions successfully estimate the capacity of the typical OV MV BPL urban class of German Reg TP NB30 and aggravated OV MV BPL urban class, respectively. In contrast, Weibull channel attenuation statistical distribution, which was the most suitable for estimating the capacity of OV MV BPL topology classes for FCC Part 15 regardless of the examined OV MV BPL topology class, remains the most suitable in OV MV BPL rural class for the capacity estimations regardless of the applied IPSD limits. However, with reference to average absolute percentage change, there is no channel attenuation statistical distribution that can successfully cope with all the OV MV BPL topology classes.
- As UN MV BPL topology classes are concerned when German Reg TP NB30 and BBC/NATO proposal are applied, Wald channel attenuation stops to support the most successful capacity estimations. When German Reg TP NB30 is assumed, Weibull and Lognormal channel attenuation statistical distributions best estimate MLEs of typical and aggravated UN MV BPL urban classes, respectively, while Gaussian channel attenuation statistical distribution best estimates the capacity of UN MV BPL suburban and rural classes. During the application of German Reg TP NB30, Lognormal channel attenuation statistical distribution is the only distribution that can successfully cope with all the examined UN MV BPL classes with respect to its below 3% average absolute percentage change. When BBC/NATO proposal is applied, capacities of typical and aggravated UN MV BPL urban classes cannot be successfully estimated by any channel attenuation statistical distribution while capacities of UN MV BPL suburban and rural classes can be best estimated by the Lognormal channel attenuation statistical distribution.

From the previous analysis, it is evident that the lower IPSD limits undermine capacity estimations of the channel attenuation statistical distributions. The most affected distribution BPL topology classes by the reduction of the IPSD limits are the OV MV BPL ones and the urban BPL topology classes regardless of the power grid type. Apart from the different EMI policies, different coupling schemes, which are supported by different coupling scheme modules, can be applied in distribution BPL networks. The impact of the different coupling schemes on the performance of channel attenuation statistical distributions of the statistical hybrid model is benchmarked in the following subsection.

2.3. Statistical Hybrid Model, Channel Attenuation Statistical Distributions and Coupling Schemes of CS2 Module

In accordance with [1, 8, 10], a coupling scheme module describes the injection of the input BPL signal onto and the extraction of the output BPL signal from the power lines of BPL networks. The general implementation of CS2 module, which is the most updated BPL coupling scheme module and applied in this paper, is illustrated in Figs. 3(a) and 3(b) of [1] while its supported coupling schemes are also reported in [8]. As already mentioned in [1], three different types of coupling schemes can be supported namely: (1) *Coupling Scheme Type 1: Wire-to-Ground (WtG)* or *Shield-to-Phase (StP)* coupling schemes for OV or UN BPL networks, respectively; (2) *Coupling Scheme Type 2: Wire-to-Wire (WtW)* or *Phase-to-Phase (PtP)* coupling schemes for OV or UN BPL networks, respectively; and (3) *Coupling Scheme Type 3: MultiWire-to-MultiWire (MtM)* or *MultiPhase-to-MultiPhase (MtM)* coupling schemes for OV or UN BPL networks, respectively. Among the available coupling schemes of coupling scheme type 1, WtG^1 and StP^1 coupling schemes have been arbitrarily chosen among the default operation settings due to their frequent and easy installation across OV and UN BPL networks, respectively. In this subsection, one representative coupling scheme per coupling scheme type and power grid type is examined, namely [10]: (i) as the coupling scheme type 2 is concerned, $\mathrm{WtW}^{1\text{-}2}$ and $\mathrm{PtP}^{1\text{-}2}$ coupling schemes are applied to OV MV and UN MV BPL topology classes, respectively; and (ii) as the coupling scheme type 3 is concerned, $\mathrm{MtM}^{1\text{-}2\text{-}3}_{0.8\_-0.1\_-0.1}$ coupling scheme is applied to MV BPL topology classes.

Since different coupling schemes entail changes in coupling scheme channel attenuation values, the MLEs of the five examined channel attenuation statistical distributions of indicative OV MV BPL topologies of Table 1 of [1] are reported in Table 6 when the default operation settings are assumed but for $\mathrm{WtW}^{1\text{-}2}$ and $\mathrm{MtM}^{1\text{-}2\text{-}3}_{0.8\_-0.1\_-0.1}$ coupling schemes of CS2 module. In Table 7, MLEs of the five examined channel attenuation distributions are reported for the indicative UN MV BPL topologies of Table 2 of [1] when the default operation settings are assumed but for $\mathrm{PtP}^{1\text{-}2}$ and $\mathrm{MtM}^{1\text{-}2\text{-}3}_{0.8\_-0.1\_-0.1}$ coupling schemes of CS2 module.

By comparing Tables 6 and 7 with Tables 1 and 2, respectively, important observations can be pointed out that describe the performance of channel attenuation statistical distributions during the operation of the statistical hybrid model for the different coupling types of CS2 module. In accordance with [10], by adopting CS2 module, WtW coupling schemes of OV MV BPL topologies and PtP coupling schemes of UN MV BPL topologies become almost equivalent to respective WtG coupling schemes and StP coupling schemes in terms of channel attenuation and capacity while MtM coupling schemes of OV MV BPL topologies and UN MV BPL topologies present slightly improved metrics in comparison with the respective ones of WtG and StP coupling schemes. Hence, MLEs of Tables 6 and 7 present close values either among them for given power grid type or to the ones of the respective Tables 1 and 2.

Apart from the coupling channel attenuation, MLEs, and capacity values, it is well known that the different coupling schemes present different EMIs for given IPSD limits. As already mentioned in [10], MtM and WtW/PtP coupling schemes with a careful selection of conductors and respective conductor participation percentages may present significantly lower EMI than the EMI of WtG/StP coupling schemes. Therefore, a careful relaxation of FCC Part 15 for MtM and WtW/PtP coupling schemes that do not create additional EMI may produce significant capacity increase and better performance of channel attenuation statistical distributions during the operation of the statistical hybrid model.

To numerically assess the performance of channel attenuation statistical distributions during the operation of the hybrid statistical model when different coupling schemes are applied, the percentage change between each average capacity of the distribution BPL topology class and the capacity of the indicative topology of the respective class for the channel attenuation distributions of Tables 6 and 7 is given in Table 8 when the default operation settings are applied but for the WtW^{1-2} and $\mathrm{PtP}^{1\text{-}2}$ coupling schemes for OV MV and UN MV BPL topology classes, respectively. Similar to Table 3, at the bottom of the table, the average percentage change of each channel attenuation statistical distribution is given per power grid type. In Table 9, same table as Table 8 is given but for the application of $\mathrm{MtM}^{1\text{-}2\text{-}3}_{0.8\_-0.1\_-0.1}$ coupling scheme for OV MV and UN MV BPL topology classes.

By comparing Tables 8 and 9 with Table 3, it is evident that the similar behavior of different coupling schemes in terms of MLEs is reflected on a similar behavior of percentage changes for given distribution BPL topology class and channel attenuation statistical distribution regardless of the selected

Table 6. Same with Table 1 but for WtW^{1-2} and $\text{MtM}^{1-2-3}_{0.8\_-0.1\_-0.1}$ coupling schemes of CS2 module. (blue: WtW coupling scheme/red: MtM coupling scheme).

Topology Name	BPL Topology Class Description	Gaussian MLEs		Lognormal MLEs		Wald MLEs		Weibull MLEs		Gumbel MLEs	
		$\hat{\mu}^{Gaussian}_{MLE}$	$\hat{\sigma}^{Gaussian}_{MLE}$	$\hat{\mu}^{Lognormal}_{MLE}$	$\hat{\sigma}^{Lognormal}_{MLE}$	$\hat{\mu}^{Wald}_{MLE}$	$\hat{\lambda}^{Wald}_{MLE}$	$\hat{\alpha}^{Weibull}_{MLE}$	$\hat{\beta}^{Weibull}_{MLE}$	$\hat{\alpha}^{Gumbel}_{MLE}$	$\hat{\epsilon}^{Gumbel}_{MLE}$
Urban case A	Typical OV MV BPL urban topology class	12.77 / 12.77	11.85 / 11.64	1.69 / 1.71	3.48 / 3.47	12.77 / 12.77	7×10^{-10} / 7×10^{-10}	12.09 / 12.17	0.86 / 0.88	19.37 / 19.22	15.58 / 14.83
Urban case B	Aggravated OV MV BPL urban topology class	17.82 / 17.84	13.80 / 13.54	2.49 / 2.51	1.03 / 0.99	17.82 / 17.84	8.20 / 9.65	19.18 / 19.32	1.27 / 1.31	25.40 / 25.26	18.01 / 17.35
Suburban case	OV MV BPL suburban topology class	7.47 / 7.48	9.91 / 9.76	0.97 / 1.03	2.73 / 2.68	7.47 / 7.48	1×10^{-9} / 1×10^{-9}	6.19 / 6.34	0.72 / 0.75	13.42 / 13.33	16.15 / 15.79
Rural case	OV MV BPL rural topology class	2.81 / 2.96	3.23 / 3.16	-0.03 / 0.21	2.64 / 2.54	2.81 / 2.96	1×10^{-9} / 1×10^{-9}	2.29 / 2.64	0.71 / 0.80	4.58 / 4.67	3.71 / 3.50
"LOS" case	OV MV BPL "LOS" transmission class	1×10^{-11} / 1×10^{-11}	4×10^{-26} / 4×10^{-26}	-25.33 / -25.33	4×10^{-15} / 4×10^{-15}	1×10^{-11} / 1×10^{-11}	2621.44 / 2621.44	1×10^{-11} / 1×10^{-11}	∞ / ∞	1×10^{-11} / 1×10^{-11}	0 / 0

Table 7. Same with Table 2 but for $\text{PtP}^{1\text{-}2}$ and $\text{MtM}^{1\text{-}2\text{-}3}_{0.8\_-0.1\_-0.1}$ coupling schemes of CS2 module. (blue: PtP coupling scheme/red: MtM coupling scheme).

Topology Name	BPL Topology Class Description	Gaussian MLEs		Lognormal MLEs		Wald MLEs		Weibull MLEs		Gumbel MLEs	
		$\hat{\mu}^{Gaussian}_{MLE}$	$\hat{\sigma}^{Gaussian}_{MLE}$	$\hat{\mu}^{Lognormal}_{MLE}$	$\hat{\sigma}^{Lognormal}_{MLE}$	$\hat{\mu}^{Wald}_{MLE}$	$\hat{\lambda}^{Wald}_{MLE}$	$\hat{\alpha}^{Weibull}_{MLE}$	$\hat{\beta}^{Weibull}_{MLE}$	$\hat{\alpha}^{Gumbel}_{MLE}$	$\hat{\epsilon}^{Gumbel}_{MLE}$
Urban case A	Typical UN MV BPL urban topology class	10.58 / 10.58	7.81 / 7.81	2.14 / 2.14	0.64 / 0.64	10.58 / 10.58	20.9 / 20.9	11.85 / 11.85	1.51 / 1.51	15.04 / 15.04	10.66 / 10.66
Urban case B	Aggravated UN MV BPL urban topology class	19.96 / 19.96	8.17 / 8.17	2.90 / 2.90	0.47 / 0.47	19.96 / 19.96	80.22 / 80.22	22.48 / 22.48	2.63 / 2.63	24.18 / 24.18	8.55 / 8.55
Suburban case	UN MV BPL suburban topology class	7.04 / 7.04	2.73 / 2.73	1.85 / 1.85	0.49 / 0.49	7.04 / 7.04	24.7 / 24.7	7.90 / 7.90	2.80 / 2.80	8.41 / 8.41	2.90 / 2.90
Rural case	UN MV BPL rural topology class	3.54 / 3.54	1.23 / 1.23	1.21 / 1.21	0.35 / 0.35	3.54 / 3.54	27.1 / 27.1	3.95 / 3.95	2.84 / 2.84	4.24 / 4.24	1.88 / 1.88
"LOS" case	UN MV BPL "LOS" transmission class	1×10^{-11} / 1×10^{-11}	4×10^{-26} / 4×10^{-26}	-25.33 / -25.33	4×10^{-15} / 4×10^{-15}	1×10^{-11} / 1×10^{-11}	2621.44 / 2621.44	1×10^{-11} / 1×10^{-11}	∞ / ∞	1×10^{-11} / 1×10^{-11}	0 / 0

coupling scheme. However, taking into account the small percentage change differences for given distribution BPL topology class and channel attenuation statistical distribution, it can be noticed that the percentage change remains inversely proportional to the capacity.

The aforementioned relation between percentage change and capacity implies that a second rule of thumb in this paper, say, a rule of thumb between the spectral efficiency and the success of a channel attenuation statistical distribution, can be proposed; for spectral efficiencies below 270 Mbps/27 MHz = 10 bps/Hz, the success of a channel attenuation statistical distribution becomes precarious. This second rule of thumb is more evident in Tables 4 and 5 where low IPSD limits are adopted. However, even if high IPSD limits of FCC Part 15 are applied, the second rule of thumb is evident in OV MV BPL topology classes of Tables 3, 8, and 9 where only one channel attenuation statistical distribution (i.e., Weibull channel attenuation statistical distribution) can successfully estimate capacities of all OV MV BPL topology classes regardless of the applied coupling scheme. Anyway, the findings that occur in Table 3 are also valid in Tables 8 and 9, say: (i) UN MV capacity estimations remain more successful than OV MV ones regardless of the applied coupling scheme, and (ii) Weibull and Wald channel attenuation statistical distributions perform the best capacity estimations in OV MV and UN MV power grid types for all the examined BPL topology classes regardless of the applied coupling scheme. Note that the

Table 8. Same with Table 3 but for $\text{WtW}^{1\text{-}2}$ and $\text{PtP}^{1\text{-}2}$ coupling schemes for OV MV and UN MV BPL topology classes, respectively.

Indicative BPL Topology Name (OV MV Capacity / UN MV Capacity in Mbps)	BPL Topology Class Description	Percentage Change (%)									
		Gaussian		Lognormal		Wald		Weibull		Gumbel	
		OV MV	UN MV	OV MV	UN MV	OV MV	UN MV	OV MV	UN MV	OV MV	UN MV
Urban case A (232 / 550)	Typical OV MV BPL urban class	-4.73	-0.52	-10.53	0.22	47.25	0.01	1.72	-0.18	-7.79	-1.27
Urban case B (193 / 465)	Aggravated OV MV BPL urban	-4.98	-0.04	3.70	-0.43	14.41	0.04	0.66	-0.04	-5.88	0.41
Suburban case (278 / 582)	OV MV BPL suburban class	-5.29	-0.01	-11.27	-0.23	23.00	0.003	-0.27	0.02	-10.38	0.23
Rural case (317 / 613)	OV MV BPL rural class	-1.02	-0.001	-10.39	-0.01	7.95	0.0005	-0.20	0.03	-1.85	0.28
Average Absolute Percentage Change (%)		**4.01**	**0.14**	**8.97**	**0.22**	**23.16**	**0.02**	**0.71**	**0.07**	**6.48**	**0.55**

Table 9. Same with Table 3 but for $\text{MtM}^{1\text{-}2\text{-}3}_{0.8\_-0.1\_-0.1}$ coupling scheme for OV MV and UN MV BPL topology classes.

Indicative BPL Topology Name (OV MV Capacity / UN MV Capacity in Mbps)	BPL Topology Class Description	Percentage Change (%)									
		Gaussian		Lognormal		Wald		Weibull		Gumbel	
		OV MV	UN MV	OV MV	UN MV	OV MV	UN MV	OV MV	UN MV	OV MV	UN MV
Urban case A (243 / 571)	Typical OV MV BPL urban class	-4.12	-0.50	-11.32	0.21	45.59	0.01	1.60	-0.17	-7.08	-1.22
Urban case B (203 / 487)	Aggravated OV MV BPL urban	-4.50	-0.04	3.00	-0.42	11.74	0.03	0.34	-0.04	-5.70	0.39
Suburban case (290 / 603)	OV MV BPL suburban class	-4.82	-0.01	-11.74	-0.22	22.30	0.003	-0.27	0.02	-9.64	0.23
Rural case (327 / 635)	OV MV BPL rural class	-0.85	-0.001	-11.43	-0.01	8.13	0.0004	-0.12	0.03	-1.57	0.27
Average Absolute Percentage Change (%)		**3.57**	**0.14**	**9.37**	**0.22**	**21.94**	**0.01**	**0.58**	**0.06**	**6.00**	**0.53**

second rule of thumb is based on the metric of spectral efficiency in order to be able to be generalized for future use in the 3–88 MHz frequency range of BPL operation.

Concluding this Section, there is no channel attenuation statistical distribution that can successfully estimate the capacity for all the BPL topology classes, but the selection of the most suitable channel attenuation statistical distribution depends on the power grid type, BPL topology class, IPSD limits, and applied coupling scheme. In general terms, Weibull and Wald channel attenuation statistical distributions perform the best capacity estimations in OV MV and UN MV power grid types when relatively high IPSD limits occur.

3. CONCLUSIONS

In this second paper, the results of the statistical hybrid model have been presented while the Gaussian, Lognormal, Wald, Weibull, and Gumbel channel attenuation statistical distributions have been benchmarked for various power grid types, BPL topology classes, IPSD limits, and coupling schemes.

Based on the theoretical framework of [1] and the findings of this paper, one of the most crucial elements during the operation of the statistical hybrid model remains the estimation of MLEs for given channel attenuation statistical distribution since it further influences the capacity estimations. The success of a capacity estimation has been examined in terms of the proposed metrics of capacity percentage change and average absolute capacity percentage change as well as the first rule of thumb. In general terms, Weibull and Wald channel attenuation statistical distributions perform the best capacity estimations in OV MV and UN MV power grids, respectively, regardless of the examined BPL topology class and the applied coupling scheme when IPSD limits remain relatively high (e.g., FCC Part 15). EMI policies that are considered as more protective to the other telecommunications services already coexisting with BPL systems are characterized by relatively lower IPSD limits (e.g., German Reg TP NB30 and BBC/NATO proposal) that foment the success of a capacity estimation. With reference to the values of capacity percentage change and average absolute capacity percentage change, as the IPSD limits become lower, a successful capacity estimation becomes more difficult creating a mixed scenario regarding the selection of the most suitable channel attenuation statistical distribution among the BPL topology classes and power grid types. In fact, the success degree of a capacity estimation is relatively proportional to the spectral efficiency of the representative indicative BPL topology of the examined distribution BPL topology class. Converse to IPSD limits, different coupling scheme types do not significantly affect the metrics of capacity percentage change and average absolute capacity percentage change for given IPSD limits and, hence, the selection of the most suitable channel attenuation statistical distribution. Concluding these two papers, the proposed statistical hybrid model can be considered as a valuable simulation tool that can define and enrich BPL topology classes with realistic BPL topology members.

REFERENCES

1. Lazaropoulos, A. G., "Statistical broadband over power lines channel modeling — Part 1: The theory of the statistical hybrid model," *Progress In Electromagnetics Research C*, Vol. 92, 1–16, 2019.
2. Lazaropoulos, A. G., "Factors influencing broadband transmission characteristics of underground low-voltage distribution networks," *IET Commun.*, Vol. 6, No. 17, 2886–2893, Nov. 2012.
3. Lazaropoulos, A. G. and P. G. Cottis, "Transmission characteristics of overhead medium voltage power line communication channels," *IEEE Trans. Power Del.*, Vol. 24, No. 3, 1164–1173, Jul. 2009.
4. Lazaropoulos, A. G. and P. G. Cottis, "Capacity of overhead medium voltage power line communication channels," *IEEE Trans. Power Del.*, Vol. 25, No. 2, 723–733, Apr. 2010.
5. Lazaropoulos, A. G. and P. G. Cottis, "Broadband transmission via underground medium-voltage power lines — Part I: Transmission characteristics," *IEEE Trans. Power Del.*, Vol. 25, No. 4, 2414–2424, Oct. 2010.
6. Lazaropoulos, A. G. and P. G. Cottis, "Broadband transmission via underground medium-voltage power lines — Part II: Capacity," *IEEE Trans. Power Del.*, Vol. 25, No. 4, 2425–2434, Oct. 2010.
7. Lazaropoulos, A. G., "Towards modal integration of overhead and underground low-voltage and medium-voltage power line communication channels in the smart grid landscape: Model expansion, broadband signal transmission characteristics, and statistical performance metrics (Invited Paper)," *ISRN Signal Processing*, Vol. 2012, Article ID 121628, 1–17, 2012, [Online]. Available: http://www.hindawi.com/isrn/sp/2012/121628/.
8. Lazaropoulos, A. G., "Broadband performance metrics and regression approximations of the new coupling schemes for distribution broadband over power lines (bpl) networks," *Trends in Renewable Energy*, Vol. 4, No. 1, 43–73, Jan. 2018, [Online]. Available: http://futureenergysp.com/index.php/tre/article/view/59/pdf.
9. Lazaropoulos, A. G., "Towards broadband over power lines systems integration: transmission characteristics of underground low-voltage distribution power lines," *Progress In Electromagnetics Research B*, Vol. 39, 89–114, 2012.
10. Lazaropoulos, A. G., "New coupling schemes for distribution broadband over power lines (BPL) networks," *Progress In Electromagnetics Research B*, Vol. 71, 39–54, 2016.
11. FCC, "In the matter of amendment of part 15 regarding new requirements and measurement guidelines for access broadband over power line systems," *FCC 04-245 Report and Order*, Jul. 2008.

12. Nutzungsbestimmungen NB30 & Reg TP 322 MV 05 Part 1, "Specification for the measurement of disturbance fields from telecommunications systems and networks in the frequency range 9 kHz to 3 GHz", *German RegTP*, Oct. 2001.
13. NATO, "HF interference, procedures and tools (interférences HF, procédures et outils) final report of NATO RTO information systems technology," *RTO-TR-ISTR-050*, Jun. 2007.
14. Lazaropoulos, A. G., "A panacea to inherent BPL technology deficiencies by deploying broadband over power lines (BPL) connections with multi-hop repeater systems," *Bentham Recent Advances in Electrical & Electronic Engineering*, Vol. 10, No. 1, 30–46, 2017.
15. Lazaropoulos, A. G., "The impact of noise models on capacity performance of distribution broadband over power lines networks," *Hindawi Computer Networks and Communications*, Vol. 2016, Article ID 5680850, 14 pages, 2016, doi:10.1155/2016/5680850. [Online]. Available: http://www.hindawi.com/journals/jcnc/2016/5680850/.
16. Lazaropoulos, A. G., "Capacity performance of overhead transmission multiple-input multiple-output broadband over power lines networks: The insidious effect of noise and the role of noise models (Invited Paper)," *Trends in Renewable Energy*, Vol. 2, No. 2, 61–82, Jun. 2016, [Online]. Available: http://futureenergysp.com/index.php/tre/article/view/23.
17. Lazaropoulos, A. G., "Review and progress towards the capacity boost of overhead and underground medium-voltage and low-voltage broadband over power lines networks: Cooperative communications through two- and three-hop repeater systems," *ISRN Electronics*, Vol. 2013, Article ID 472190, 1–19, 2013, [Online]. Available: http://www.hindawi.com/isrn/electronics/aip/472190/.
18. Lazaropoulos, A. G., "Smart energy and spectral efficiency (SE) of distribution broadband over power lines (BPL) networks — Part 1: The impact of measurement differences on SE metrics," *Trends in Renewable Energy*, Vol. 4, No. 2, 125–184, Aug. 2018, [Online]. Available: http://futureenergysp.com/index.php/tre/article/view/76/pdf.
19. Lazaropoulos, A. G., "Smart energy and spectral efficiency (SE) of distribution broadband over power lines (BPL) networks — Part 2: L1PMA, L2WPMA and L2CXCV for SE against measurement differences in overhead medium-voltage BPL networks," *Trends in Renewable Energy*, Vol. 4, No. 2, 185–212, Aug. 2018, [Online]. Available: http://futureenergysp.com/index.php/tre/article/view/77/pdf.
20. Lazaropoulos, A. G., "Designing broadband over power lines networks using the techno-economic pedagogical (TEP) method — Part I: Overhead high voltage networks and their capacity characteristics (Invited Review Article)," *Trends in Renewable Energy*, Vol. 1, No. 1, 16–42, Mar. 2015, [Online]. Available: http://futureenergysp.com/index.php/tre/article/view/2.
21. Lazaropoulos, A. G., "Overhead and underground MIMO low voltage broadband over power lines networks and EMI regulations: Towards greener capacity performances," *Elsevier Computers and Electrical Engineering*, Vol. 39, 2214–2230, 2013.
22. Fenton, D. and P. Brown, "Some aspects of benchmarking high frequency radiated emissions from wireline communications systems in the near and far fields," *Proc. IEEE Int. Symp. on Power Line Communications and its Applications*, 161–167, Malmö, Sweden, Apr. 2001.
23. Gebhardt, M., F. Weinmann, and K. Dostert, "Physical and regulatory constraints for communication over the power supply grid," *IEEE Commun. Mag.*, Vol. 41, No. 5, 84–90, May 2003.
24. NTIA, "Potential interference from broadband over power line (BPL) systems to federal government radio communications at 1.7–80 MHz Phase 1 Study Vol. 1," NTIA Rep. 04-413, Apr. 2004.
25. Milioudis, A., G. Andreou, and D. Labridis, "Optimum transmitted power spectral distribution for broadband power line communication systems considering electromagnetic emissions," *Elsevier Electric Power Systems Research*, Vol. 140, 958—964, 2016, DOI: 10.1016/j.epsr.2016.03.047.